

Elaboration and Electrochemical Studies of the Coating Behavior of a New Nanofunctional Epoxy Polymer on E24 Steel in 3.5 % NaCl

Rachid Hsissou^{a,*}, Bouchra Benzidia^b, Najat Hajjaji^b and Ahmed Elharfi^a

^aLaboratory of Agro-resources, Polymers and Process Engineering (LAPPE), Team of Organic Chemistry and Polymers (TOCP), Department of Chemistry, Faculty of Sciences,

Ibn Tofail University, P.O. Box 133, 14000, Kénitra, Morocco

^bLaboratory of Materials, Electrochemistry and Environment, Team of Corrosion, Protection and Environment, Department of Chemistry, Faculty of Sciences, Ibn Tofail University, P.O. Box 133, 14000, Kénitra, Morocco

Received February 13, 2017; accepted, December 2, 2017

Abstract

The goal of our work is to develop, study, characterize and apply new epoxy macromolecular matrices in the coating process, and to optimize them in the conservation of marine heritage. Epoxy resins are technologically and nanotechnologically compatible thermosetting macromolecule matrices, which are easy to use, thanks to their structures and viscosimetric and rheological properties, able to protect the heritage subject to atmospheric corrosion. In this paper, we tested the synthesized, crosslinked and formulated novel macromolecular nanoglycidyl trihydrazine 4,4,4-tripropoxy ethylene tribisphenol A (NGTHTPETBA), used as an anti-corrosive coating for E24 steel in 3.5% NaCl. In order to evaluate the inhibiting performance of the NGTHTPETBAE coating for E24 steel corrosion, and to examine its coating behavior, we applied the different E₁(NGTHTPETBA/MDA) and E₂(NGTHTPETBA/MDA/PN) formulations. The stationary and transient electrochemical studies are very revealing.

Keywords: NGTHTPETBA, coating, E24 steel, adsorption phenomenon, crosslinking, formulation and electrochemical studies.

Introduction

Polyepoxide resins are very important thermosetting technological macromolecular matrices [1- 2], which have been widely used in several industrial fields, such as radioactive waste conditioning [3-4], viscosimetric and rheological behavior [5-6-7], aeronautical construction [8], spatial construction [9-10], and metallic objects corrosion inhibition [11] and coating [12]. Our goal

* Corresponding author. E-mail address: r.hsissou@gmail.com

is to assess a new behavior of an E24 steel coating, which is easy to implement and inexpensive for the heritage protection subjected to standard atmospheric corrosion. The field of heritage conservation has borrowed some corrosion protection means that were developed for industrial applications, such as the so-called chemical or electrochemical conversion coatings, metallic deposits or organic polymer films, which are now commonly used. As a result, these processes have been used in the field of heritage conservation. This study consists in physico-chemically applying and studying a new polyepoxide resin, and its anticorrosive behavior against E24 steel in marine environments. These materials can be corroded in aggressive media [13-14] and, therefore, the best way to protect them against corrosion is a coating application [15-16]. Among these various types of coatings we have found organic polymers, which play a very important role in preventing the oxidation corrosion, and also avoiding the heritage degradation [17-18]. The coating method with epoxy resins remains a very effective approach to avoid rapid corrosion, because of its good adhesion, good acid/alkali resistance, and its high cross-linking density, thanks to its macromolecular structure [19].

In this work, we applied a new nanofunctional epoxy prepolymer, nanoglycidyl trihydrazine 4,4,4-tripropoxy of ethylene tribisphenol A, synthesized in the laboratory [20], on E24 steel, in marine environments. The coating impact on E24 steel was assessed by using the two E₁ (NGTHTPETBA/MDA) and E₂ (NGTHTPETBA/MDA/PN) protection formulations, while evaluating their anti-corrosive behavior by two electrochemical methods, namely the stationary method and the transitional method.

Materials and methods

Hardware

Used products

In this work, we used the nanofunctional epoxide prepolymer nanoglycidyl trihydrazine 4.4.4-tripropoxy of ethylene tribisphenol A (NGTHTPETBA), synthesized in the laboratory [20], methylene dianiline (MDA), natural phosphate and 3.5 % NaCl. The latter has been marketed by Aldrich Chemical Co.



Figure 1. The electrochemical cell with three electrodes.

Used methods

Electrochemical cell with three electrodes

Electrochemical measurements were obtained by using an electrochemical cell with three electrodes, as shown in Fig. 1.

There is a platinum electrode as a counter electrode, a saturated calomel reference electrode (ECS) and a cylindrical E24 steel working electrode. The surface of contact with the corrosive solution was 1 cm². Before each test, the working electrode was polished with abrasive papers: 600, 1200 and 1500.

These three electrodes were immersed in a 100 mL container, and inserted in its orifices with well-designed diameters and spacings, making it possible to receive the systems for agitation, temperature control, aeration and deaeration.

Electrochemical measurements

By using a potentiometer/galvanostat SP-200 Biologic Science Instruments, the stationary measurements were carried out in a potentiodynamic mode. The working electrode was previously kept immersed at the free corrosion potential for 30 minutes. The scanning speed was 1 mV/s. The determination of the electrochemical parameters (i_{corr} , E_{corr} , β_a and β_c) from the polarization curves was carried out by using a nonlinear regression by the Ec-Lab software. Therefore, the coating efficiency was calculated through the following formula:

$$\eta \% = \left(\frac{i_{\text{corr}}^0 - i_{\text{corr}}}{i_{\text{corr}}^0} \right) \times 100 \quad (1)$$

where i_{corr}^0 and i_{corr} are the corrosion current densities (A.cm⁻²), respectively, without and with the coating polymer's different formulations.

β_a and β_c are the Tafel constants of the anodic and cathodic reactions (V⁻¹), respectively. These constants are related to the slope of Tafel β (V.dec⁻¹) and the form on the logarithmic scale given by:

$$\beta = \frac{\ln(10)}{b} = \frac{2.303}{b} \quad (2)$$

The electrochemical impedance spectroscopy measurements were carried out by using the same apparatus, with a signal amplitude of 10 mV. The explored frequency ranged from 100 KHz to 10 MHz. The results were then analyzed by using an equivalent electrical circuit of Bouckamp simulation program [19]. The effectiveness of the coating protection was evaluated by using the following relationship:

$$\eta \% = \left(\frac{R_p - R_p^0}{R_p} \right) \times 100 \quad (3)$$

where R_p^0 and R_p are the polarization resistance, respectively, in the absence and presence of the coating polymer's different formulations.

The hardening of nanoglycidyl trihydrazine 4,4,4-tripropoxy of ethylene tribisphenol A (NGTHTPETBA)

The polyepoxide resins can be converted into thermosetting macromolecular matrices, because many of their chemical compounds function as curing agents during the process. Among the hardeners of polyepoxide systems, there are two major classes: acid anhydrides and amines. The latter remain good hardeners thanks to their chemical structure. The aromatic compounds provide very good thermal stability and mechanical properties to the polymer [21]. They are often used for high-tech applications. The hardener which we are using is methylene dianiline, of which chemical structure is shown in Fig. 2:

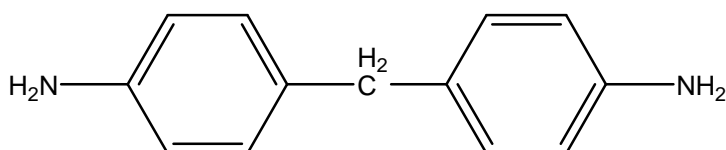


Figure 2. Semi-developed formula of methylene dianiline.

The impact of methylene dianiline on the epoxide is described by the following reaction, according to Fig. 3:

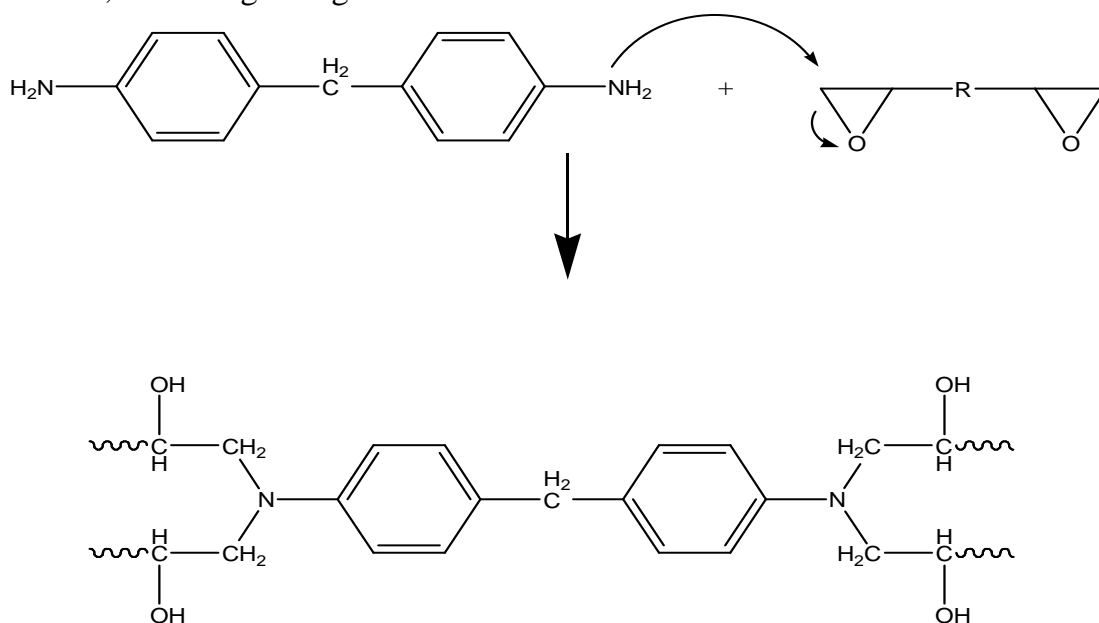


Figure 3. Diagram of NGTHTPETBA resin crosslinked with MDA.

Ratio calculation

Calculation of stoichiometric coefficients

Once having cured the multifunctional polyepoxide macromolecular matrix in the hardener presence (especially amines), in order to obtain its optimum properties, it is desirable to make the prepolymer and the curing agent react to approximately stoichiometric amounts [7].

Calculation of the epoxy equivalent (EEW) to the synthesized nanoglycidyl trihydrazine 4,4,4-tripropoxy of ethylene tribisphenol A macromolecular matrix is as follows:

$$EEW = \frac{M_w(NGTHTPETBA)}{f} \quad (4)$$

with f as the functionality of the synthesized epoxy resin, where:

$$EEW = \frac{1486}{9} \quad (5)$$

$$EEW = 165 \text{ g / eq} \quad (6)$$

The calculated AHEW (Amine Hydrogen Equivalent Weight) constitutes the mass of the hardener containing an amine equivalent.

$$AHEW = \frac{M_w(MDA)}{f} \quad (7)$$

Methylene dianiline: $M_w = 198$; $f = 4$

$$AHEW = \frac{198}{4} \quad (8)$$

$$AHEW = 49.5 \text{ g / eq} \quad (9)$$

Calculation of the ratio by weight

The hardener-resin ratio by weight was calculated, in the majority of cases, per PHR (parts per hundred of resin):

$$A \text{ min } e(PHR) = \frac{AHEW}{EEW} \times 100 \quad (10)$$

In this case, for NGTHTPETBA:

$$A \text{ min } e(PHR) = \frac{49.5}{165} \times 100 \quad (11)$$

$$A \text{ min } e(PHR) = 30 \text{ g / eq} \quad (12)$$

Therefore, 30 g of methylene dianiline per 100 g of nanoglycidyl trihydrazine 4,4,4-tripropoxy of ethylene tribisphenol A had to react with the prepolymer, curing it, for it to achieve optimum properties.

Calculation of the load quantity

We calculated the quantity of the desired load according to the following equation:

$$y\% = \frac{x}{re \sin + MDA + x} \quad (13)$$

E24 steel metal coating by nanoglycidyl trihydrazine 4,4,4-tripropoxy of ethylene tribisphenol A

To obtain reliable and reproducible results, the plate was subjected, before each test, to the surface polishing with abrasive papers of increasingly fine grain sizes: 600, 1200 and 1500. The used experimental protocol is as follows: Formulation 1 (NGTHTPETBA/MDA) - we mixed 1 g of NGTHTPETBA with 0.3 g of MDA, as a hardener, and then stirred it to give a single fluid phase for about 30 min. The formulation was applied to E24 steel by using a film-producing rod. This coated plate was placed in the oven at 70 °C for 24 hours, to crosslink the polymer deposited onto the substrate; Formulation 2 (NGTHTPETBA/MDA/PN) - we followed the previous protocol (Formulation 1) with the addition of 5% of natural phosphate as load.

The used electrolyte (3.5% NaCl)

We used 3.5% NaCl as a corrosive solution. We prepared 100 mL of 3.5 % NaCl, and then we dissolved 3.5 g of it in 100 mL of distilled water. The used polyepoxide resin was NGTHTPETBA.

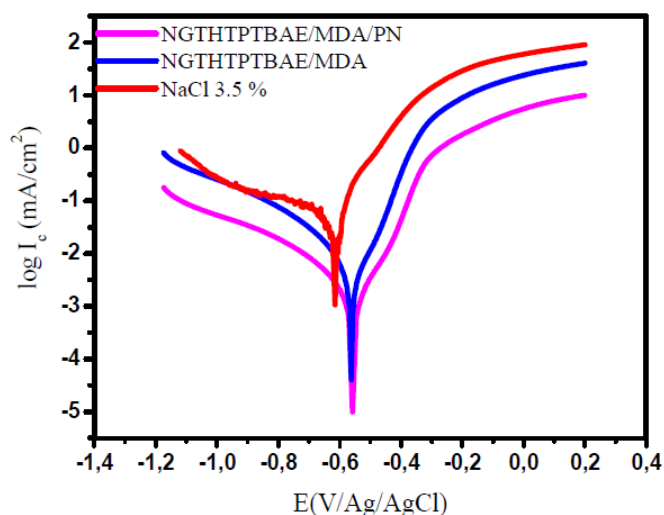


Figure 4. Polarization curves of E24 steel in 3.5% NaCl, in the presence of the matrices (E_0 , E_1 and E_2), after 30 min of immersion at 298 K.

In Fig. 4, we notice that the cathodic branches do not show linearity, and are considered to be the sum of two curves (showing mixed kinetics) by reducing oxygen and hydrogen [22]. However, the anodic branches also do not show linearity, due to the E24 steel dissolution [23].

Table 1. Accumulations of the various electrochemical parameters recorded from the polarization curves.

Protective matrices	Plaques (E _i)	- E _{corr} (mV/Ag/AgCl)	I _{corr} (μA/cm ²)	β _c (mV/dec)	β _a (mV/dec)	η (%)
3.5 % in NaCl	E ₀	665	22	275	78	-
NGTHTPETBA/MDA	E ₁	562	1.98	82	80	91
NGTHTPETBA/MDA/PN	E ₂	558	0.80	110	98.5	96

In this section, we have studied the protecting mechanism for E24 steel by the matrices (E₀, E₁ and E₂), which consist of the standard polyepoxide resin (NGTHTPETBA), the hardener (MDA) and the natural phosphate load. The results interpretation, according to the matrix constitution, is as follows:

In the control E₀ matrix, which was made without the substrate coating, the Cl⁻ and OH⁻ anions coming from the corrosive medium directly attack the substrate, which induces direct corrosion.

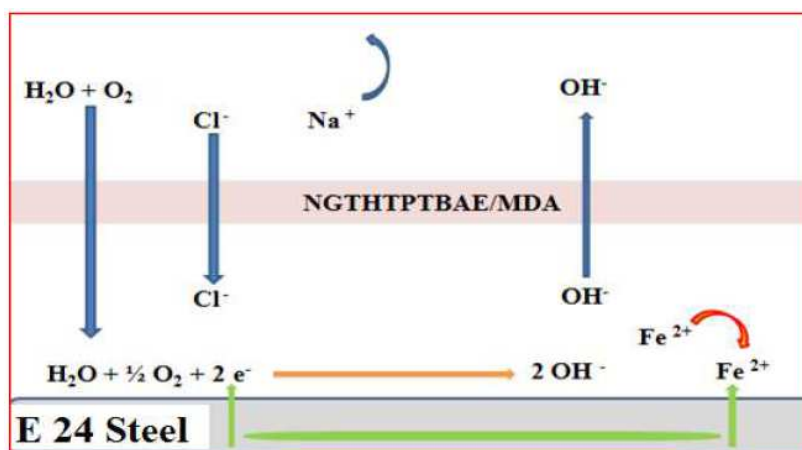


Figure 5. Mechanism of the E₁ protective matrix (NGTHTPTBAE/MDA) amid the metal substrate and the film, after immersion in 3.5% NaCl.

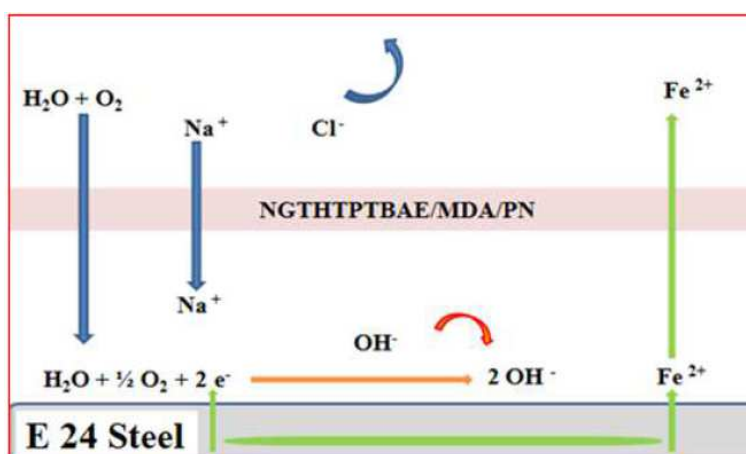


Figure 6. Protective mechanism of the E₂ matrix (NGTHTPETBA/MDA/PN) amid the metal substrate and the film, after immersion in 3.5% NaCl.

Fig. 5 and 6 show the protection mechanism for E24 steel by the E₁ (NGTHTPETBA/MDA) and E₂ (NGTHTPETBA/MDA/PN) formulations, respectively without and with the natural phosphate.

Thanks to the E₁ matrix (NGTHTPETBA/MDA), we anticipate that there is a relatively large diffusion of chloride and hydroxyl ions through the protective film, which could have micropores, by inducing the primary corrosion, translated by $i_{\text{corr}} = 1.98 \mu\text{A}/\text{cm}^2$ and $\eta\% = 91\%$. This would lead to an acceleration of the metal anodic dissolution [24]. The E₁ matrix protection mechanism is shown in Fig. 5.

Once having applied E₂ matrix (NGTHTPETBA/MDA/PN), we have found that the corrosive species (Cl^- and OH^-) diffusion is slowed down by the layer formed by natural phosphate [25-26]. In this case, the electrochemical corrosion parameters are $i_{\text{corr}} = 0.80 \mu\text{A}/\text{cm}^2$ and $\eta = 96\%$. The protection mechanism for the E₂ matrix is shown in Fig. 6.

The corrosion potential mainly moves towards the anode direction, with E₁ (NGTHTPETBA/MDA) and E₂ (NGTHTPETBA/MDA/PN) matrices. The addition of 5% of natural phosphate is accompanied by a marked decrease in corrosion current, in both cathodic and anodic domains. This allowed us to conclude that natural phosphate addition to the formulation made it act as a mixed inhibitor.

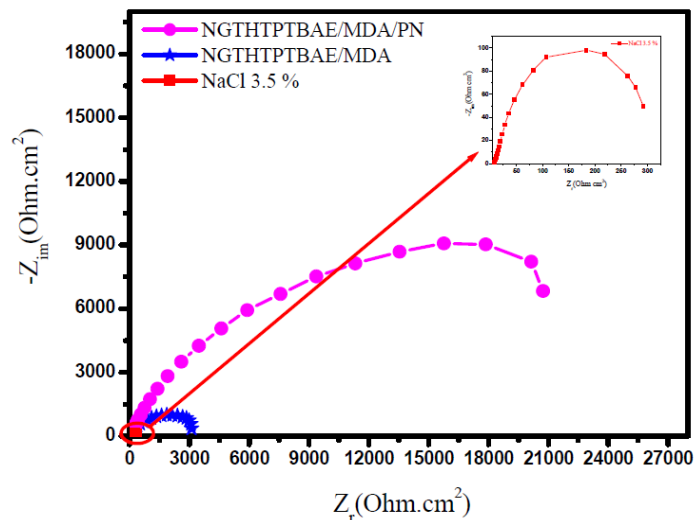


Figure 7. Open-circuit electrochemical impedance diagrams after immersing E24 steel in 3.5% NaCl, in the matrices (E₀, E₁ and E₂) presence, at 298 K.

Electrochemical impedance spectroscopy

In order to study in detail the mechanism of coating behavior, we performed electrochemical impedance spectroscopy, of which results are represented in the form of Nyquist diagrams. These impedance diagrams of the E24 steel, immersed 30 min before each open circuit measurement in the corrosive 3.5 % NaCl solution, with respect to the set of matrices (E₀, E₁ and E₂), are presented in Fig. 7. This confirms the results obtained by the potentiodynamic polarization curves. The analysis of the different diagrams on the composition of the protective matrices (E₀, E₁ and E₂) shows that they are formed by a high-frequency

capacitive loop attributed to the film effect, which is due to the diffusion phenomenon. In fact, the more the semi-circle diameter increases, the better is the corrosion resistance of the protective film [27]. This study confirms the results obtained by the stationary method.

Furthermore, Fig. 8 and 9, respectively, show the Bode and the phase angle patterns of the E24 steel coating behavior in a marine environment. The plots of these diagrams in the presence of different formulations, E₀, E₁ and E₂, are illustrated in the figures below.

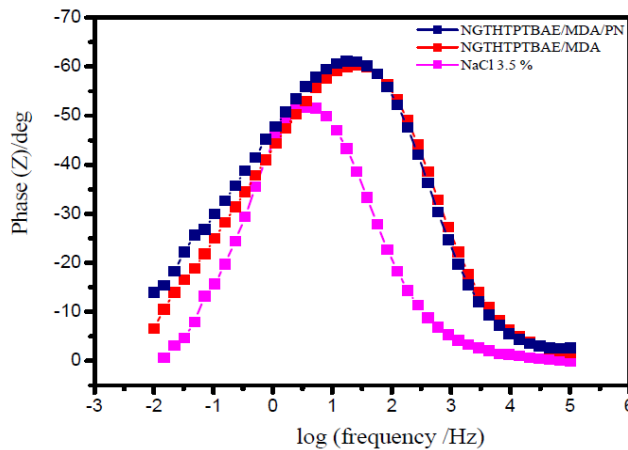


Figure 8. Phase angle diagrams of NGTHTPETBA in 3.5% NaCl, after 30 min of immersion in different formulations (E₀, E₁ and E₂) at 298 K.

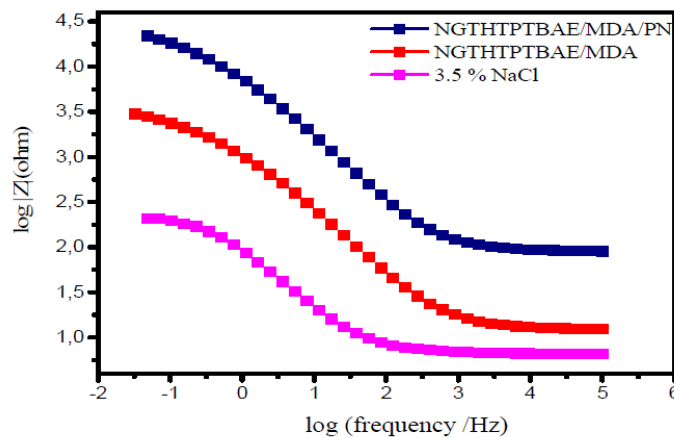


Figure 9. Bode diagrams of NGTHTPETBA in 3.5% NaCl, after 30 min of immersion in different formulations (E₀, E₁ and E₂), at 298 K.

According to Fig. 8, we have found that the phase angles increased with the number of coating constituents. This increase in phase angles confirms a higher protection obtained by stronger coating formulations (E₀, E₁ and E₂). Indeed, from this phase angle diagram, we have found that there are three frequency domains: low frequencies, high frequencies and intermediate frequencies. For low frequencies, the increase in the impedance absolute values confirms the greatest protection with different coating formulations for E24 steel. At high frequency, the phase angle values are approximately equal to zero. This indicates that the electrode behavior corresponds to the solution resistance [28]. For the

intermediate frequencies, the phase angle is close to 70° , and a linear relationship between $\log |Z|$ in view of $\log (f)$, with a slope close to -1, was observed. The latter shows the capacitive behavior of the coating at intermediate frequencies.

In the literature, the condenser's behavior would be ideal, if the slope value reached -1, and if a phase angle value reached 90° . The phase angle values are calculated from the phase curves (Z) in view of \log (frequency). These values of α vary between -0.50 and -0.70 for the different coating formulations, which could be related to the non-ideal structure of the metal/solution interface. These results confirm those of electrochemical impedance spectroscopy.

According to the presented curve shapes, the Bode and Nyquist diagrams show a capacitive behavior at the interface, and the existence of an equivalent electrical circuit (Fig. 10), which is due to the interpretation of the information on the behavior properties of the metal surface coating or corrosion. This circuit is composed of: R_s (electrolyte resistance); C_f (coating film capacity); R_p (coating film resistance); R_{ct} (load transfer resistor); and C_{dl} (double layer capacity).

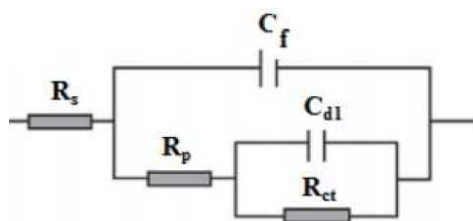


Figure 10. Equivalent electrical circuit of the impedance diagrams obtained in the presence of different formulations for E24 steel in 3.5% NaCl.

The electrochemical impedance values and the efficiency resulting from each protection matrix (E_0 , E_1 and E_2) are grouped in Table 2.

Table 2: Various electrochemical parameters taken from the impedance diagrams.

Protective matrices E_i	R_s ($\Omega.cm^2$)	R_{ct} ($\Omega.cm^2$)	C_{dl} ($\mu F/cm^2$)	C_f ($\mu F/cm^2$)	R_p ($\Omega.cm^2$)	η (%)
E_0	6.5	2.40	1253	935	218.6	-
E_1	12	5	236	11.4	3519	94
E_2	84.9	31.8	34	1.94	29346	99

From this table, we conclude that the polarization resistance values of the coating film for the E_0 , E_1 and E_2 protective matrices confirm the parameters results obtained from the potentiodynamic polarization curves. Table 3 summarizes the results of the stationary and transient methods.

Table 3. Evaluation parameters of the stationary and transient methods.

E_i	stationary method		transient method	
	I_{corr} ($\mu A/cm^2$)	η (%)	R_p ($\Omega.cm^2$)	η (%)
E_0	22	-	218.6	-
E_1	1.98	91	3519	94
E_2	0.80	96	29346	99

That behavior is correlated with a very low barrier effect caused by the existence of pores and defects in the coating, and/or by the poor adhesion between the coating and the metal substrate. The absence of adhesion of the non-pigmented coatings is suggested by the obtained low charge transfer resistance and the rapid formation of bubbles over the entire coating surface, where the significant corrosion occurs [29]. On this basis, the larger semi-circle in the E₂ coating system Nyquist diagram indicates a better corrosion resistance (see Table 3), which is explained by the presence of a natural phosphate responsible for the higher corrosion resistance.

Conclusion

After synthesizing the nanofunctional polyepoxide prepolymer nanoglycidyl trihydrazine 4,4,4-tripropoxy of ethylene tribisphenol A, we applied it for E24 steel protection by a coating process, which is derived from the formulations based on a standard epoxy prepolymer, methylene dianiline and natural phosphate used as a load. The obtained electrochemical results, namely the potentiodynamic polarization curves and those of the electrochemical impedance spectroscopy, are quite in reasonable agreement, and confirm that the natural phosphate presented in the formulated E₂ matrix (NGTHTPETBA/MDA/PN) has a strong protective effect. Finally, the Bode and the phase angle diagrams confirm the electrochemical impedance spectroscopy results. In perspective we will approach the theoretical modeling study by using the DFT and the PM6 methods, in order to confirm the adhesion sites onto the metal support.

References

1. Fetouaki S, Toufik M, Meghraoui H, et al. *Phys Chem New J.* 2006;27:131-140.
2. Hsissou R, El Rhayam Y, Elharfi A. *Int J Innov Appl Stu.* 2014;7:674-682.
3. Bekhta A, Lambarki El Alliou T, Bouih A, et al. *Int J Innov Appl Stu.* 2014;7:1057-1070.
4. El Hilal B, Elharfi A. *Int J Innov Appl Stu.* 2014;7:729-735.
5. Hsissou R, Dagdag O, El Harfi A. *Mor J Chem.* 2015;3:791-797.
6. Hsissou R, El Harfi A. *Mor J Chem.* 2016;4:315-323.
7. Hsissou R, Bekhta A, El Harfi A. *J Mater Environ Sci.* 2017;8:603-610.
8. Grich M, Meghraoui H, Ziraoui R, et al. *Ann Chim Sci Mat.* 2011;36:1-10.
9. El Azzaoui J, El-Aouni N, Bekhta A, et al. *Mor. J. Chem.* 2015;3:338-345.
10. Hsissou R, El Harfi A. *Int J Phar Tech Res.* 2017;10:Accepted.
11. Dagdag O, El Gouri M, Galai M, et al. *Der Pharm Chem.* 2015;7:114-122.
12. Dagdag O, Galai M, Ebn Touhami M, et al. *J Mater Environ Sci.* 2016;7:3454-3464.
13. Nakamura Y, Yamaguchi M, Okubo M, et al. *J Appl Polym Sci.* 1992;45:1281-1289.
14. Rosales B, Vera R, Morien G. *Corros Sci.* 1999;41:625-651.
15. Cantor A, Bushman J, Glodoski M, et al. *Mater Performance.* 2006;45:38-41.

16. Antonijevic MM, Petrovic MB. *Int J Electrochem Sci.* 2008;3:1-28.
17. Petitjean J, Aeiyaeh S, Lacroix JC, et al. *J Electroanal Chem.* 1999;478:92-100.
18. Panah NB, Danaee I. *Prog Org Coat.* 2010;68:214-218.
19. Ferreira CA, Aeiyaeh S, Delamar M, et al. *Chem Interfacial Electrochem.* 1990;284:351-369.
20. Hsissou R, Bekhta A, El Hilal B, et al. *Int J Sci Eng Res.* 2017;8:1181-1188.
21. Hsissou R, Rafik M, Hegazi SE, et al. *Arab J Chem Envir Res.* 2016;3:35-50.
22. Li W, Hu L, Zhang S, et al. *Corros Sci.* 2011;53:735-745.
23. Hammouti B, Dafali A, Touzani R, et al. *J Saudi Chem Soc.* 2012;16:413-418.
24. Zubielewicz M, Gnot W. *Prog Org Coat.* 2004;49:358-371.
25. Rossenbeck B, Ebbinghaus P, Stratmann M, et al. *Corros Sci.* 2006;48:3703.
26. Liu S, Zhong Y, Jiang R, et al. *Corros Sci.* 2011;53:746.
27. Ananda Kumar S, Balakrishnan T, Alagar M, et al. *Prog Org Coat.* 2006;55:207.
28. Benali O, Larabi L, Traisnel M, et al. *Appl Surf Sci.* 2007;253:6130-6139.
29. Guillaumin V, Landolt D. *Corros Sci.* 2002;44:179.